In situ defect annealing of swift heavy ion-irradiated CeO_2 and ThO_2*

Raul I. Palomares[1,#], *Cameron L. Tracy*[2], *Fuxiang Zhang*[2], *Changyong Park*[3], *Dmitry Popov*[3], *Christina Trautmann*[4,5], *Rodney C. Ewing*[6], *Maik Lang*[1,]

[1]University of Tennessee, Knoxville, TN, U.S.A.; [2]University of Michigan, Ann Arbor, MI, U.S.A.; [3]Geophysical Laboratory, Carnegie Institution of Washington, Argonne, IL, U.S.A.; [4]GSI Helmholtzzentrum & Technische Universität Darmstadt, Germany; [6]Stanford University, Stanford, CA, U.S.A.

Ceria (CeO_2) and thoria (ThO_2) are isostructural analogues to typical nuclear fuels, such as UO_2. During reactor operation, nuclear fuels are exposed to intense radiation fluxes and temperature gradients. These conditions, in particular fission fragment- and fast neutron-fluxes, generate nanoscale defects and induce adverse effects such as swelling and redox reactions [1]. Such modifications can degrade materials properties relevant to fuel performance.

In this study [2], a hydrothermal diamond anvil cell (HDAC) and synchrotron x-ray diffraction (XRD) configuration was used to investigate the defect annealing kinetics in swift heavy ion-irradiated CeO_2 and ThO_2 at ambient pressure. Swift heavy ions were used to simulate the effect of ionizing fission-fragment irradiation because of the similarity in specific kinetic energies (>1 MeV/nucleon) and energy deposition mechanisms.

Polycrystalline CeO_2 and ThO_2 cold-pressed pellets were irradiated at room temperature at the M2-beamline of the UNILAC of GSI with 945 MeV ^{197}Au ions to a fluence of 2.5×10^{13} ions-cm^{-2}. After irradiation, the samples were transferred into one of two holes that were drilled into a rhenium gasket (Fig. 1) for use with an HDAC. In order to monitor the recovery kinetics of ion-induced defects in CeO_2 and ThO_2, the samples were isochronally annealed for 20 minutes per step in 50-75 K temperature steps from 300-1075 K at beamline 16-BM-D of the Advanced Photon Source, U.S.A.. After each heating step, the samples were quenched to ambient temperature and allowed to equilibrate for 20 minutes. Upon reaching stable temperature, diffraction patterns were recorded.

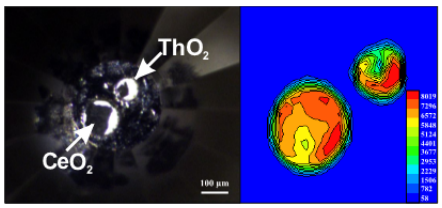

Fig. 1: The HDAC sample chamber as imaged by light microscopy (left) and x-ray absorption (right).

* This work was supported as part of the Materials Science of Actinides, an Energy Frontier Research Center funded by the US DOE Office of Science, Office of Basic Energy Sciences under Award Number DE-SC0001089..
# rpalomar@utk.edu

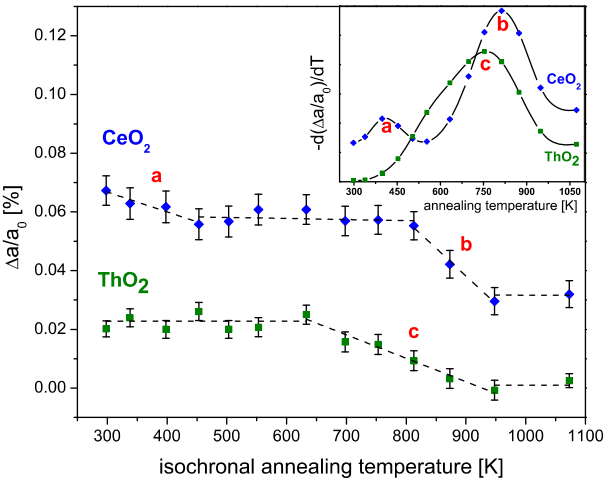

Fig. 1: Fig. 2: The relative change in the unit cell parameter, a, from the unirradiated value, a_0, as a function of isochronal annealing temperature. The inset shows the differential curves of the data.

Irradiation induces unit cell expansion due to the accumulation of isolated point defects which can agglomerate into defect clusters. As a material is heated, these defects are annealed and the unit cell parameter begins to recover. The annealing data indicate that the materials recover at different rates. The differential curves show one defect recovery stage in ThO_2 while there exist two in CeO_2 within the temperature regime investigated (Fig. 2 inset).

Material recovery was attributed [2] to the relaxation of heterogeneous microstrain, and the recombination and annihilation of anion defects (*a* & *c*, Fig. 2). This is followed by cation vacancy migration in CeO_2 (*b*, Fig. 2). The discrepancy in kinetics can be attributed to the redox behavior exhibited by CeO_2 under energetic irradiation [1]. These results suggest that cation electronic configuration plays a significant role in not only the defect production behavior, but also the defect recovery mechanisms of the fluorite-structure oxides.

References

[1] C.L. Tracy *et al.*, *Redox response of actinide materials to highly ionizing radiation.* Nat Commun, 2015. **6**: p. 6133.

[2] R.I. Palomares *et al.*, *In Situ Defect Annealing of Swift Heavy Ion Irradiated CeO_2 and ThO_2*, under review

DOI:10.15120/GR-2015-1-APPA-MML-MR-06